Publ. Astron. Soc. Aust., 1998, 15, 267–72

Identification of Two $z \sim 3 \cdot 8$ QSOs in a Deep CCD Survey

Ian Smail[1,2], Alastair C. Edge[2] and Richard S. Ellis[3]

[1]School of Physics, University of New South Wales, NSW 2052, Australia
[2]Department of Physics, University of Durham, South Road, Durham, DH1 3LE, UK
Ian.Smail@durham.ac.uk

[3]Institute of Astronomy, Madingley Rd, Cambridge, CB3 0 HA, UK

Received 1998 April 2, accepted 1998 August 24

Abstract: We present the identifications of two $z \sim 3 \cdot 8$ quasars from a deep *UBI* imaging survey with the Palomar 5·1 m Telescope. The survey covers an area of 0·25 degree^2 around a sample of ten $z = 0 \cdot 2$–$0 \cdot 3$ luminous X-ray clusters. The QSOs were identified on the basis of their stellar morphologies, relatively blue optical and very red UV–optical colours. The two objects are Q 1322+5034, with total magnitudes of $B = 20 \cdot 8$, $I = 18 \cdot 3$ and $(U–B) > 4 \cdot 7$, and Q 1722+3211, which has total magnitudes of $B = 21 \cdot 8$, $I = 19 \cdot 7$ and $(U–B) > 3 \cdot 2$. Subsequent spectroscopic observations with the 4·2 m William Herschel Telescope have confirmed the identity of these two sources as QSOs at $z = 3 \cdot 82$ and $z = 3 \cdot 73$ respectively. Our spectroscopic observations identify a damped Lyman-α absorber in the spectrum of Q 1322+5034 at $z = 3 \cdot 439$, as well as a second absorption system at $z = 2 \cdot 700$, which may be either a single very high column density, damped Lyman-α system, or more likely a blend of a number of high column-density absorbers spread over a distance of ∼10 Mpc.

Keywords: cosmology: observations — cosmology: early universe — quasars: clusters

1 Introduction

Although now overtaken as the most distant objects known (Dey et al. 1998; Hu, Cowie & McMahon 1998), QSOs remain the brightest optical sources found in the distant universe, and they can therefore be used to study the structure and characteristics of gas along their sight-lines (e.g. Liske & Webb 1997). While QSOs are relatively numerous at $z \sim 2$, their numbers drop significantly at higher redshifts, $z \gtrsim 3$–4 (Shaver et al. 1998). At the time of writing there are roughly 90 $z > 3 \cdot 7$ QSOs catalogued in NED*, selected using a variety of techniques. Of these, around 10 have been detected as X-ray sources and ∼10–20 are identified as radio sources.

* The NASA/IPAC Extragalactic Database (NED) is operated by the Jet Propulsion Laboratory, California Institute of Technology, under contract with the National Aeronautics and Space Administration.

In this communication we present the identification of two $z \sim 3 \cdot 8$ QSOs, found during a deep CCD survey of moderate-redshift clusters. The two QSOs lie in the fields of A1758 ($z = 0 \cdot 280$) and A2261 ($z = 0 \cdot 225$) and they were identified as candidate high-redshift sources from their stellar morphologies, relatively blue optical colours and very red UV–optical colours. Their redshifts have subsequently been confirmed from spectroscopic observations. In the next section we present the observations of these two objects before going on to discuss their observed properties. Throughout we assume $\Omega_0 = 1$ and $H_0 = 50\,\mathrm{km\,s^{-1}\,Mpc^{-1}}$.

2 Observations

We begin by discussing the photometric data used to identify the two QSO candidates, as well as archival information on these sources, before detailing our spectroscopic observations, which have confirmed that both objects are high-redshift QSOs.

1323-3580/98/030267$05.00

https://doi.org/10.1071/AS98267 Published online by Cambridge University Press

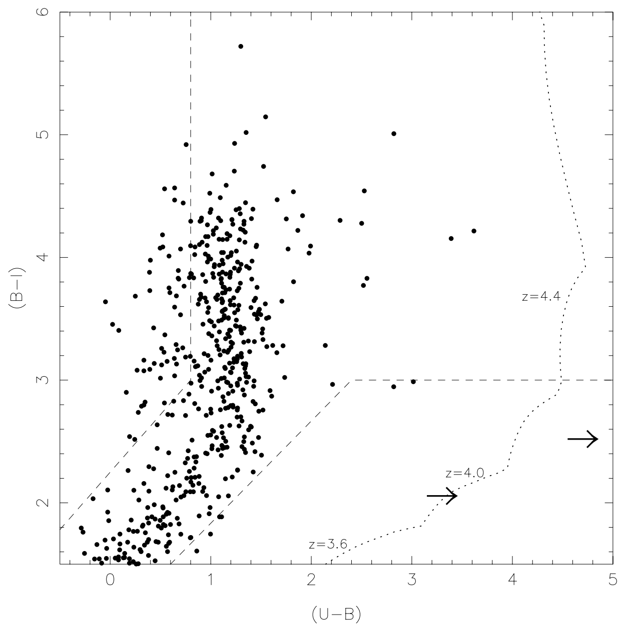

Figure 1—The $(U-B)$–$(B-I)$ colour–colour plot for the $I < 21$ objects with stellar morphologies from the combined fields of S98. The two QSOs are remarkable for their relatively blue $(B-I)$ and very red $(U-B)$ colours, and are marked as lower limits on this plot. The dotted line shows the expected colours of a QSO with a UV spectral slope of ν^{α}, with $\alpha = 0{\cdot}5$, as a function of redshift. This prediction includes the effects of blanketing by the Lyman-α (Madau 1995). The structure in this locus arises from the approximations used in the blanketing estimate. We also show the rough boundaries of the region in the colour–colour plane within which stars fall (taken from the distribution in Landolt 1992).

2.1 Palomar Observations

The details of the observations and analysis of a CCD survey undertaken with the Hale 5·1 m Telescope of the Palomar Observatory* are given in Smail et al. (1998, S98) and we provide only a very brief overview here. The aims of the survey were to study the galaxy populations of the clusters and to catalogue candidate lensed features within their cores (Edge et al. 1998, E98). The survey consists of deep UBI imaging of $9{\cdot}7 \times 9{\cdot}7$ arcmin regions centred on ten $z = 0{\cdot}2$–$0{\cdot}3$ luminous X-ray clusters selected from the ROSAT All-sky Survey. The imaging discussed here was acquired under good conditions during the nights of 1994 June 9–12, using the COSMIC imaging spectrograph (Kells et al. 1998) and a thinned, blue-sensitive 2048^2 TEK detector. The total exposure times were 500 s in both B and I and 3000 s in U, reaching an 80% completeness limit of $I \sim 22{\cdot}5$ and photometry of these detections in UB with 20% accuracy to $U \sim 25{\cdot}1$ and $B \sim 25{\cdot}9$. This survey is thus slightly deeper than that discussed in Hall et al. (1996), although their survey covers an area a little over 3 times larger than that used here (our survey covers 0·25 degree) and also includes much more extensive photometric information.

The seeing measured off the I frames discussed in this paper was 1·05 arcsec FWHM, with UB frames having typical seeing of $\sim$1·2 arcsec. Observations of Landolt (1992) provide photometric calibration of the observations. Standard reduction techniques were applied to the science frames and objects were then detected and characterised from the final stacked I frames using the SExtractor package (Bertin & Arnouts 1996), with colours measured in 3 arcsec diameter aperture from the seeing-matched frames. The estimated reddenings in the two fields discussed here are $E(B-V) = 0{\cdot}02$ for A1758 and $E(B-V) = 0{\cdot}07$ for A2261 and no reddening corrections have been applied to any of the photometry presented.

As part of the calibration and analysis, we produced $(U-B)$–$(B-I)$ colour–colour plots of those objects with $I < 21$ that some were classed as stars on the basis of their ellipticities and FWHM. 621 objects were selected from the complete survey covering 0·25 square degrees. For bright samples these plots show a strong stellar track, which allowed us to confirm the accuracy of our photometric observations (S98). This procedure highlighted two stellar sources that were well-detected in our B and I frames with relatively blue colours, $(B-I) \sim 2{\cdot}5$, but had only upper limits to their fluxes in the U-band ($U \gg 25$, Table 1 and Figure 1). Visual inspection of the CCD frames confirmed that these two objects are bright in the BI frames, but are undetected in our deep U frames (Figure 2).

* Based on observations obtained at Palomar Observatory, which is owned and operated by the California Institute of Technology.

https://doi.org/10.1071/AS98267 Published online by Cambridge University Press

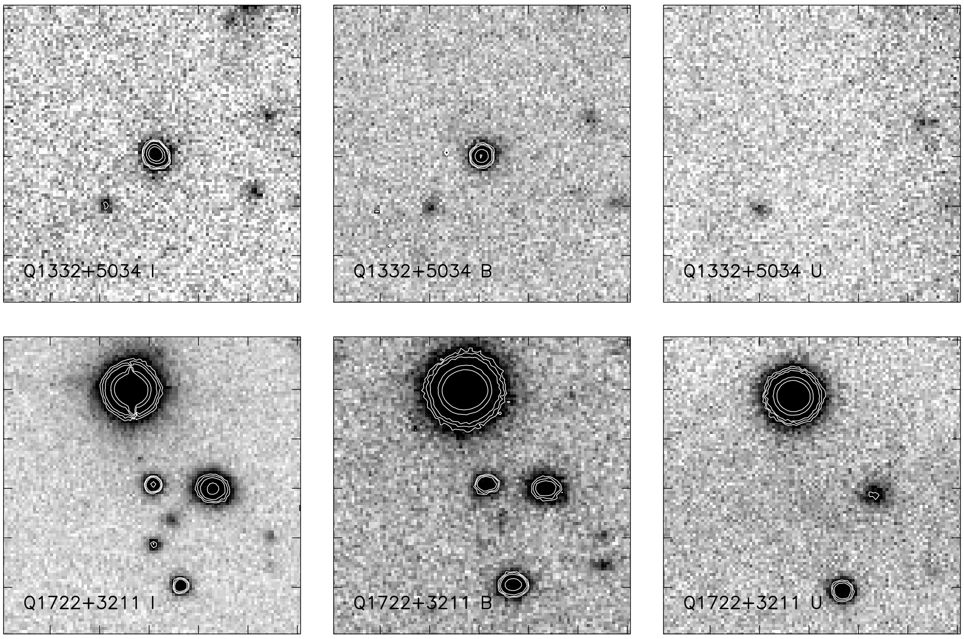

Figure 2—Deep CCD imaging of a 30×30 arcsec regions around the two QSOs. The individual panels show the regions in the three passbands UBI. The strong detections of both Q1722+3211 and Q1322+3211 in I contrast with their non-detection in the U band to $U\gtrsim 25\cdot 5$. The tick marks are every 5 arcsec on the panels and all have North top and East to the left.

Table 1. Properties of QSOs

	Q 1332+5034	Q 1722+3211	
α(J2000)	$13^{\rm h}32^{\rm m}23\cdot 2^{\rm s}$	$17^{\rm h}22^{\rm m}37\cdot 4^{\rm s}$	Position from I image,
δ(J2000)	$+50^\circ 34'32''$	$+32^\circ 11'19''$	accurate to ± 1 arcsec
r (Mpc)	$1\cdot 80$	$1\cdot 13$	Projected distance from cluster centre
z	$3\cdot 815\pm 0\cdot 002$	$3\cdot 727\pm 0\cdot 007$	
$I_{\rm tot}$	$18\cdot 33\pm 0\cdot 01$	$19\cdot 67\pm 0\cdot 02$	Total magnitude
$U_{\rm ap}$	$>25\cdot 7$	$>25\cdot 3$	1σ limits, aperture magnitude
$B_{\rm ap}$	$21\cdot 00\pm 0\cdot 01$	$22\cdot 12\pm 0\cdot 01$	Aperture magnitude
$I_{\rm ap}$	$18\cdot 43\pm 0\cdot 00$	$19\cdot 78\pm 0\cdot 01$	Aperture magnitude
$(U-B)_{\rm ap}$	$>4\cdot 7$	$>3\cdot 2$	Aperture colour (1σ limit)
$(B-I)_{\rm ap}$	$2\cdot 57\pm 0\cdot 02$	$2\cdot 34\pm 0\cdot 03$	Aperture colour
f_X ($0\cdot 1$–$2\cdot 4$ keV)	$(2\cdot 6\pm 0\cdot 5)\times 10^{-14}$	$<2\cdot 1\times 10^{-14}$	X-ray flux in erg cm^{-2} s^{-1} (10^{-3} W m^{-2})
$f_{\rm radio}$ (20 cm)	$<1\cdot 0$	$<1\cdot 0$	Radio flux in mJy

Madau (1995) showed that due to blanketing in U by the Lyman-α forest at rest-frame wavelengths shortward of 1215 Å, a flat-spectrum source at $z>3$ will have $(U-B)>2\cdot 5$, and for $z\sim 3\cdot 5$ would have $(U-B)\sim 4$–5 and $(B-I)\sim 2\cdot 5$ (see also Hall et al. 1995). Thus the very red $(U-B)$ colours for the two sources suggest that they lie at $z\gtrsim 3\cdot 5$, while their relatively blue $(B-I)$ colours indicate that the Lyman-limit has not moved completely through the B-band (Smith et al. 1994), providing an upper limit to their redshifts of $z\lesssim 4$–$4\cdot 5$. These redshift limits, combined with the compact morphologies of the two sources, support their identifications as QSOs at $z\sim 3\cdot 5$–4. The first candidate, Q 1332+5034, lies on the outskirts of the cluster A1758 ($z=0\cdot 280$), while the other, Q 1722+3211, lies in the field of A2261 ($z=0\cdot 225$). The large projected radii of the two sources in these clusters means that they are not significantly gravitationally amplified, with amplifications expected to be $A\sim 1\cdot 1$.

2.2 Archival Data

By virtue of their presence in the fields of luminous X-ray clusters, we have observations of the sources at X-ray wavelengths from the ROSAT X-ray satellite. A 16 ks HRI image of A2261 provides only an upper limit for the X-ray flux of Q 1722+3211 (Table 1). However, the 29 ks HRI observation of A1758 shows that Q 1332+5034 is coincident with an unresolved X-ray source with a flux $f(0\cdot 1$–$2\cdot 4\,{\rm keV})=(2\cdot 6\pm 0\cdot 5)\times 10^{-14}$ erg cm^{-2} s^{-1} (unabsorbed, assuming a power-law index of $1\cdot 5$).

We have also searched the $1\cdot 4$ GHz VLA FIRST survey (White et al. 1997) for radio emission associated with the two QSOs. We find no detectable

https://doi.org/10.1071/AS98267 Published online by Cambridge University Press

emission in the FIRST survey for Q 1332+5034 or Q 1722+3211. These upper limits correspond to a rest-frame 7·1 GHz (4·3 cm) power of less than $1{\cdot}2 \times 10^{26}$ W Hz^{-1}, so neither object can be classed as radio-loud.

2.3 Spectroscopic Observations

The spectroscopic observations of the two QSO candidates were undertaken during an observing run to spectroscopically confirm the nature of a number of weak and strongly lensed background sources identified in the cluster fields (E98). Details of these observations can be found in E98, and we repeat some of that material here. The observations were obtained on the nights of 1997 July 4–6 with the ISIS dual-beam spectrograph on the 4·2 m William Herschel Telescope (WHT) on La Palma.

Using the 158 line mm^{-1} gratings in both the red and blue arms provides 2·9 Å pixel^{-1} sampling and ~8 Å resolution with a 1·5 arcsec slit, across a continuous wavelength range from 3500–9000 Å. Conditions during the run were good, with a median seeing of 0·9 arcsec and good transparency. The total exposure times were 1200 s for Q 1332+5034 and 600 s on Q 1722+3211. Standard IRAF reduction procedures were used to process both the science frames and calibration data. We show the fluxed spectra of the two QSOs in Figure 3.

3 Analysis and Discussion

We identify strong, broad emission lines associated with Lyα λ1216, Lyβ λ1026, Si IV λ1397 and C IV λ1549 in the spectra of both QSOs (Figure 3). Observed wavelengths, equivalent widths and FWHM

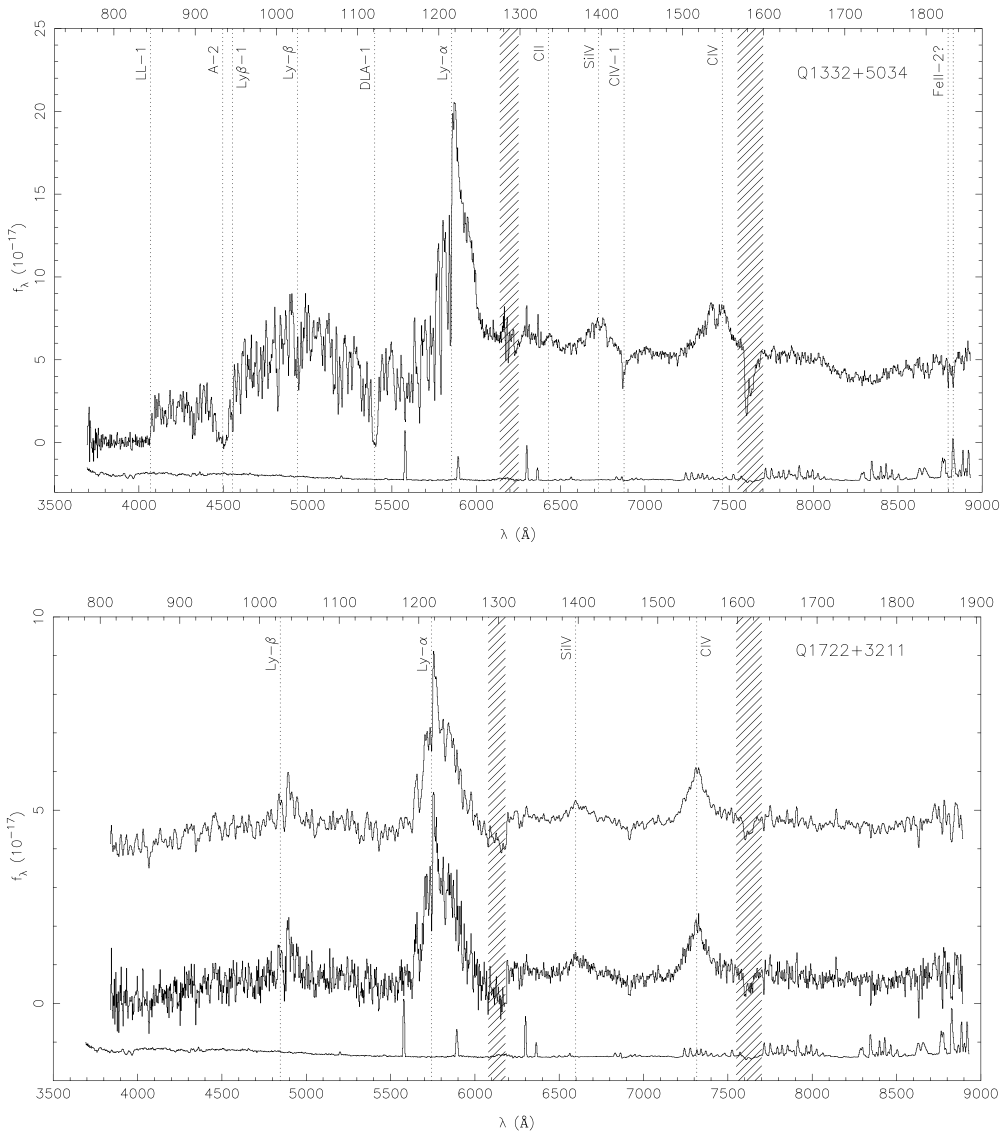

Figure 3—The spectra of Q1332+5034 and Q1722+3211 obtained with ISIS on the WHT. Each panel shows the fluxed spectrum of the source, as well as an arbitrarily scaled spectrum of the night sky. In addition, in Q1722+3211, we also show at the top the spectrum smoothed to the instrumental resolution. The identifications of the main features are shown in both spectra (Table 2). In Q1332+5034 the features marked with –1/–2 are associated with the foreground absorption systems. The lower scale on each plot gives the observed wavelengths, while the upper scale indicates the wavelengths in the rest frame of the QSO. The hatched regions mark areas affected by atmospheric absorption or the dichroic of the spectrograph.

https://doi.org/10.1071/AS98267 Published online by Cambridge University Press

Table 2. Catalogue of spectral features

ID	λ	z	$\mathrm{EW_{obs}}$ (Å)	$\mathrm{FWHM_{obs}}$ (Å)	Comment
			Q 1332+5034		
Lyα	5871 ± 2	$3 \cdot 828$	—	—	Peak of flux, not used in z estimate
Lyβ	4943 ± 10	$3 \cdot 818$	—	—	Not used in z estimate
SiIV	6727 ± 2	$3 \cdot 815$	-33 ± 2	120 ± 20	
CIV	7459 ± 2	$3 \cdot 815$	-109 ± 5	200 ± 10	Blended with A-band
DLA–1 Lyα	5398 ± 2	$3 \cdot 439$	58 ± 5	55 ± 5	Damped Ly-α
DLA–1 Ly-limit	4063 ± 5	$3 \cdot 446$	—	—	Lyman-limit for DLA–1
DLA–1 CIV	6877 ± 2	$3 \cdot 439$	6 ± 1	17 ± 5	
A–2 Lyα	4496 ± 2	$2 \cdot 700$	135 ± 5	128 ± 5	Damped Ly-α or blend?
			Q 1722+3211		
Lyα	5754 ± 2	$3 \cdot 732$	—	—	Peak of flux, not used in z estimate
Lyβ	4897 ± 5	$3 \cdot 773$	—	—	Not used in z estimate
CIV	7315 ± 2	$3 \cdot 722$	-210 ± 10	130 ± 10	Blended with A-band
SiIV	6612 ± 2	$3 \cdot 732$	-60 ± 5	120 ± 5	

of the lines were measured interactively with the IRAF task SPLOT; these are all listed in Table 2. From the SiIV and CIV lines we estimate the redshifts of the two QSOs as $z = 3 \cdot 815 \pm 0 \cdot 002$ and $z = 3 \cdot 727 \pm 0 \cdot 007$, for Q 1332+5034 and Q 1722+3211 respectively.

Using the redshifts calculated above, we estimate luminosities of $M_B \sim -28 \cdot 3$ for Q 1332+5034 and $M_B \sim -26 \cdot 8$ for Q 1722+3211. At these redshifts their modest apparent magnitudes, compared to other $z \sim 4$ QSOs, mean that these two sources are roughly an order of magnitude less luminous than the median luminosity of known $z \sim 4$ QSOs. The observed X-ray flux of Q 1322+5034 represents a luminosity of $L_X = (3 \cdot 0 \pm 0 \cdot 6) \times 10^{45}$ erg s^{-1} in the $0 \cdot 5$–$11 \cdot 6$ keV band.

The spectrum of Q 1332+5034 shows a number of strong absorption features shortward of Lyman-α emission in the QSO. These include at least three relatively strong features within 100 Å (5000 km s^{-1}) of the peak of the Lyman-α emission in the QSO. Similar 'associated' absorbers are commonly seen in radio and X-ray-bright QSOs. However, the more interesting absorbers are further to the blue; the first of these, DLA–1, is at 5398 Å and we identify this as a damped Lyman-α absorber at $z = 3 \cdot 439$. This system completely obscures the background QSO at wavelengths below 912 Å in its rest frame and also produces detectable CIV and Ly-β absorption (Figure 3).

Identifying the lower-redshift absorption system in the spectrum of Q 1332+5034 with Lyman-α absorption gives its redshift as $z \sim 2 \cdot 70$. This feature is extremely strong, with a rest-frame equivalent width of 35 Å, and if formed from a single absorption system would indicate a column density of around $\log N(\mathrm{HI}) \sim 21 \cdot 5$–$22 \cdot 0$. Some support for this identification comes from the tentative detection of FeII $\lambda 2383$ and FeII $\lambda 2374$ at the extreme red end of our spectrum, although these coincide with strong atmospheric emission. However, the absorption profile shows only marginal evidence for broad damping wings (Figure 3), which should be easily visible for such a high column density. We suggest, therefore, that the feature most probably arises from a blend of a number of individual Lyman-α absorbers. The absorbers would need to be spread over a velocity range of ~5000 km s^{-1}. This relatively broad velocity range implies that this system is unlikely to be a collapsed structure (cf. Ortiz-Gil et al. 1997), but is more likely to be an over-dense region consisting of several high column density systems. For the observed velocity range at $z \sim 2 \cdot 7$ these could be spread over a region as large as 10–15 Mpc.

Clusters of strong absorption systems similar to A–2 are relatively rarely seen, the system in PKS 2000−330 (Carswell et al. 1987) being another, although that does not span as wide a velocity range as the system in Q 1332+5034. Therefore, irrespective of its precise interpretation, A–2 is an intriguing system and hence worthy of more detailed study.

4 Conclusions

We have identified two candidate $z \sim 4$ QSOs on the basis of their UV and optical colours and stellar morphologies from a multi-colour CCD survey covering $0 \cdot 25$ square degrees to $I = 21$.

Spectroscopic observations of the two candidates confirm that they are QSOs: Q 1332+5034 at $z = 3 \cdot 815$ and Q 1722+3211 at $z = 3 \cdot 727$. Q 1332+5034 is coincident with a faint X-ray source.

Our spectra also show two strong absorption systems along the line-of-sight to Q 1332+5034. The more distant of these is a damped Lyman-α system at $z = 3 \cdot 439$, which also produces a Lyman-limit in the QSO spectrum.

The second, lower-redshift absorption system in Q 1332+5034 at $z \sim 2 \cdot 70$ has an observed equivalent width of ~130 Å, and thus arises either from an extremely high column density damped Lyman-α absorber or from a blend of several strong absorbers. We favour the second interpretation and thus suggest that this feature may represent an over-dense region in the Lyman-α forest with a co-moving size of $\sim$10 Mpc. Such structures appear to be rare and we conclude that Q 1332+5034 is worthy of more detailed scrutiny.

Acknowledgments

IRS and ACE acknowledge the award of a PPARC Advanced Fellowship and a Royal Society Fellowship respectively. This paper was written while IRS was on an Honorary Visiting Fellowship at the University of New South Wales, with additional support through a grant from the Royal Society and the Australian Research Council. We thank John Webb for his constructive comments and insight, which motivated this paper. We acknowledge useful conversations and help from Alberto Fernandez-Soto, Paul Hewitt and Jochen Liske.

References

Bertin, E., & Arnouts, S. 1996, A&AS, 117, 393
Carswell, R. F., Webb, J. K., Baldwin, J. A., & Atwood, B. 1987, ApJ, 319, 709
Dey, A., Spinrad, H., Stern, D., Graham, J. R., & Chaffee, F. H. 1998, ApJL, 498, 93
Edge, A. C., Smail, I., Ellis, R. S., Blandford, R. D., Ebeling, H., Allen, S. W., et al. 1998, MNRAS, submitted (E98)
Hall, P. B., Osmer, P. S., Green, R. F., Porter, A. C., & Warren, S. J. 1996, ApJ, 462, 614
Hu, E. M., Cowie, L. L., & McMahon, R. G. 1998, ApJL, 502, 99
Kells, W., Dressler, A., Sivaramakrishna, A., Carr, D., Koch, E., Epps, H., et al. 1998, PASP, submitted
Landolt, A. U. 1992, AJ, 104, 340
Liske, J., & Webb, J. K. 1997, in Structure and Evolution of the IGM from QSO Absorption Lines, ed. P. Petitjean & S. Charlot (Paris: Nouvelles Frontieres)
Madau, P., 1995, ApJ, 441, 18
Ortiz-Gil, A., Lanzetta, K. M., & Webb, J. K. 1997, in Structure and Evolution of the IGM from QSO Absorption Lines, ed. P. Petitjean & S. Charlot (Paris: Nouvelles Frontieres)
Shaver, P. A., Hook, I. M., Jackson, C. A., Wall, J. V., & Kellermann, K. I. 1998, in Highly Redshifted Radio Lines, ed. C. Carilli et al. (San Franscisco: ASP)
Smail, I., Edge, A. C., Ellis, R. S., & Blandford, R. D. 1998, MNRAS, 293, 124 (S98)
Smith, J. D., Djorgovski, S. G., Thompson, D., Brisken, W. F., Neugebauer, G., Matthew, K., et al. 1994, AJ, 108, 1147
White, R. L., Becker, R. H., Helfand, D. J., & Gregg, M. D. 1997, ApJ, 475, 479